Available online at www.sciencedirect.com
ScienceDirect
International Journal of Thermal Sciences 48 (2009) 747–760
International Journal of Thermal Sciences
www.elsevier.com/locate/ijts

Adaptation of the FLASH method to the measurement of the thermal conductivity of liquids or pasty materials

R. Coquard *, B. Panel

Centre Thermique de Lyon (CETHIL), UMR CNRS 5008, Domaine Scientifique de la Doua, INSA de Lyon, Bâtiment Sadi Carnot, 9 rue de la physique, 69621 Villeurbanne Cedex, France

Received 16 October 2007; received in revised form 13 June 2008; accepted 13 June 2008

Available online 7 July 2008

Abstract

This study proposes a modification of the well-known FLASH method in order to adapt it measurements on liquids or pasty materials. The new experimental procedure requires a suitable cylindrical receptacle filled with the sample to analyze. A classical FLASH measurement is applied to this receptacle. However, as the presence of the container disturbs the conductive transfer during the transient heating of the sample, we have recourse to an identification procedure, which takes into account the disturbing influence of the receptacle to compute the thermal conductivity of the material. The modified experimental apparatus as well as the identification procedure are described in detail. Thereafter, an exhaustive estimation of the measurement accuracy is performed. The measurement uncertainty proves to be lower than 4%. Finally, we applied our method to different liquid or pasty media. A good agreement is found between the experimental results obtained and the thermal conductivity indicated in the literature for these materials.
© 2008 Elsevier Masson SAS. All rights reserved.

Keywords: Thermal conductivity; FLASH method; Liquids; Pasty materials; Identification procedure

1. Introduction

The FLASH technique, which was firstly proposed by Parker et al. [1], has become one of the most widely used method of measurement of the thermal characteristics of materials (thermal diffusivity, thermal conductivity ...). Several authors have conducted general studies on the method such as Parker [1], Degiovanni [2], Degiovanni et al. [3] or Taylor [4,5]. It presents several advantages compared with the other classical methods of measurement of the thermal conductivity. Indeed, as the measurement is made during a transient heating, its duration is noticeably lower than the classical guarded hot-plate method based on steady-state measurements. Moreover, the size of the sample required is relatively limited and a small amount of material is sufficient.

The method was first developed for measurements on isotropic purely conductive solid samples and it is, at present, mainly used on this kind of materials. Different authors have proposed some modifications of the method in order to apply it to other peculiar materials:

- Degiovanni et al. [6], Krapez et al. [7], Lafond-Huot and Bransier [8], Luc and Balageas [9], and Philippi et al. [10] studied the applications of the method to anisotropic materials.
- Batsale et al. [11–13] applied it to complex heterogeneous media.
- Batsale et al. [14–16] applied it to porous materials.
- André and Degiovanni [17], Lazard et al. [18], and Hahn et al. [19] adapted it to semi-transparent materials.

However, the use of the FLASH method to measure the thermal diffusivity of liquid or doughy materials is more problematic as it is not possible to obtain a rigid sample on which the FLASH measurement is applied.

Moreover, the accurate measurement of thermal transport in liquids is a particularly difficult task due primarily to two major difficulties: convective heat transport is difficult to eliminate and radiation may be important in transparent liquids. That is

* Corresponding author. Tel.: +33 04 72 43 84 74.
E-mail address: remi.coquard1@insa-lyon.fr (R. Coquard).

1290-0729/$ – see front matter © 2008 Elsevier Masson SAS. All rights reserved.
doi:10.1016/j.ijthermalsci.2008.06.005

Nomenclature

a	thermal diffusivity	$m^2\,s^{-1}$
C	specific heat	$J\,kg^{-1}\,K^{-1}$
D_{bubble}	diameter of the bubble	m
e	thickness of the caps	m
h	global heat transfer coefficient	$W\,m^{-2}\,K^{-1}$
h_{conv}	convective heat transfer coefficient	$W\,m^{-2}\,K^{-1}$
k	thermal conductivity	$W\,m^{-1}\,K^{-1}$
l	thickness of air bubble	m
L	thickness of the sample	m
nR	number of spatial discretization along the radial axis	
nZ	number of spatial discretization along the z-axis	
N	number of experimental data	
$\vec{q}_t, \vec{q}_r, \vec{q}_c$ and $\vec{q}_{conv}$	total, radiative, conductive and convective heat flux density	$W\,m^{-2}$
$\dot{Q}$	heat flux per surface unit due to FLASH irradiation	$W\,m^{-2}$
r	radial coordinate	m
R_{max}	radius of the sample	m
R_{plex}	internal radius of the Plexiglas circlet	m
t	time	s
T	temperature	K
T_s	temperature of external surfaces	K
T_{ext}	external temperature	K
Th	bubble height	m
$\vec{u}_r$	unit vector for the radial coordinate	
$\vec{u}_z$	unit vector for the axial coordinate	
z	axial coordinate	m

Greek symbols

χ	penetration length of the FLASH irradiation	m
ε	global emissivity of the external surfaces of the container	
$\Delta\varphi$	polar angle of air bubble	rad
ρ	density	$kg\,m^{-3}$
σ_{SB}	Stefan–Boltzmann constant ($\approx 5.67 \cdot 10^{-8}$)	$W\,m^{-2}\,K^{-4}$
φ	coordinate related to the polar angle	rad
τ	duration of the FLASH irradiation	s
ν	unreeling speed of the recording paper	$m\,s^{-1}$

Subscripts

al	of aluminium
ana	analytical
exp	experimental
sam	of the sample
num	numerical
plex	of Plexiglas

Superscripts

k	at the kth iteration level
t	at time level t

the reason why, for such materials, peculiar methods must be used to measure the thermal diffusivity. These include steady-state methods such as the method of coaxial cylinder and the method of parallel plates, or transient methods, mainly the hot-wire method. However, some particular conditions have to be performed in these methods in order to avoid the problems previously mentioned for liquids due to radiation and convection. A comprehensive review of the main methods used for the measurement of the thermal conductivity of fluids is given in [20].

Despite this, some authors have already tried to adapt the FLASH method to measurement on liquids [21–26]. As a matter of fact, it may be a desirable method for measurement of the conductivity of liquids since the effect of convective heat transport could be greatly reduced by using a horizontally mounted specimen with the heat pulse impinging on the top. Schriempf [21] was the first to develop a peculiar apparatus dedicated to measurement on liquids and applied it successfully to liquid mercury. He used a container made of insulating material. The surface of liquid was covered with a transparent plate of quartz. He measured the temperature rise at the back surface of the liquid as in the original method proposed by Parker et al. [1]. However, its method is not adapted to liquids with low thermal conductivity since the heat flow through the container is no more negligible and thus, the heat flow is no more one-dimensional. Farooq et al. [22] proposed a similar approach based on a three-layered cell using an original sample holder made of outside layers brazed to a ring-shaped central spacer. They manage to estimate the thermal conductivity of water. Maeda et al. [23] also proposed a special cell in which the liquid in sandwiched between an upper and a lower platinum crucible, to provide a three-layered sandwich. They applied a curve-fitting method using a three-layer analysis with a correction for the radiative component based on the transparent body assumption. At last, Nishi et al. [24] studied the possibility to measure the thermal diffusivities of molten metals at high temperature with a laser flash method. To do that, they developed a simple cell and estimated theoretically the effect of the radiative and conductive heat losses at the interface between the molten metals. This permits them to analyze the experimental uncertainty. They concluded that their newly developed laser flash apparatus allows measuring the diffusivity of molten Nickel with an uncertainty $\pm 3\%$. However, all these studies, based on classical laser FLASH measurements, assumed that the heat transfer through the special cells or sample holders remain one-dimensional although this may not be the case. Indeed, the newly developed test devices are made of several components with variable thermal properties which can cause edge effects. That is the reason why the use of their apparatus for the measurement on liquids with thermal conductivity noticeably different from that of the container might not lead to accurate results since the heat flow is then no more one-dimensional.

To avoid this difficulty, Tada et al. [25] proposed a method based on appropriate sample geometry. They sandwiched the

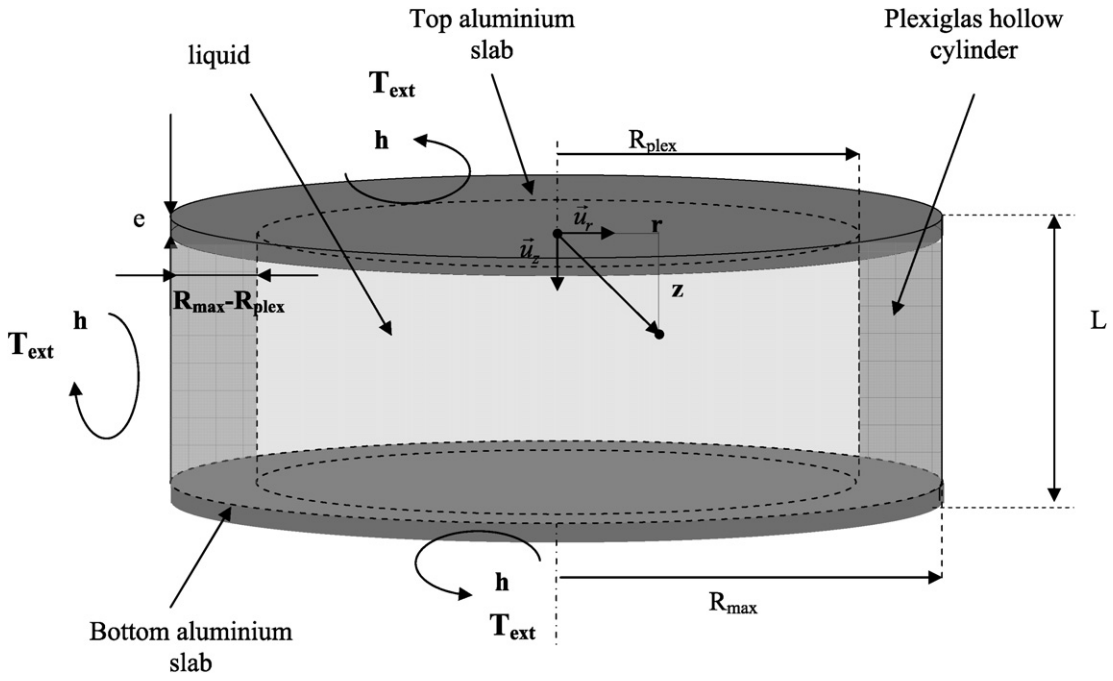

Fig. 1. Representation of the original container and of the coordinate system.

liquid between a metal plate and a sample holder and measured the evolution of the temperature on the front face, from which they obtained the conductivity of the liquid. Their method does not require neither the use of reference materials nor the measurement of the thickness of the sample since the liquid layer is regarded as a semi-infinite layer. They applied their method successfully on water and toluene. Ohta et al. [26] used a nearly identical method to measure the thermal effusivity of highly viscous liquids at high temperature. However, these original methods requiring the measurement of the temperature rise of the front face have involved the development of special measuring devices, which are not easily available.

The aim of the current work is to overcome these problems encountered when ones applies the classical (measurement at the rear face) and modified (measurement at the front face) FLASH techniques to liquids. To do that, we have developed a method very similar to the classical FLASH technique which uses an original identification procedure taking into account the perturbation of the heat transfer caused by the sample device. Besides, the main advantage of the method proposed is that it only requires the fabrication of a suitable receptacle of known dimensions and composition which is adapted to classical FLASH devices. Moreover, it allows a rapid measurement. This new procedure could find applications for the measurements of numerous materials such as biological tissues (muscle, organs, blood ...) or food materials (meat, yogurt, cheese, food gels ...) for which other classical measuring methods are not suitable.

2. Modified FLASH apparatus

We have seen that classical FLASH measurements could not be applied to liquid or pasty materials given that it requires a sample with given and immoveable dimension and shape. The previous studies mentioned in the introduction that used the classical FLASH method have surmounted this problem by developing original receptacles allowing to contain the medium during the measurement. We have built on this idea by constructing sample containers in which the sample tested could be introduced and its thermal diffusivity measured.

Each container is made of a Plexiglas hollow cylinder closed at its tops and bottoms by circular aluminium slabs (see Fig. 1). The external radius of the Plexiglas cylinder is $R_{max} = 0.015$ m which corresponds to the standard radius of classical sample tested. We choose to use Plexiglas for the material composing the hollow cylinder as its thermophysical properties ($k_{plex} = 0.19$ W/m/K, $\rho_{plex} = 1180$ kg/m^3 and $C_{plex} = 1400$ J/kg/K, $a_{plex} \approx 10^{-7}$ m^2/s) are the same order of magnitude as the ones of most of common materials tested. Consequently, the disturbing influence of the sample container on the thermal heat transfer is minimized. Similarly, the internal radius R_{plex} must be as large as possible in order to reduce the influence of the Plexiglas on the measurement. Finally, we choose aluminium for the material of the top and bottom slabs given that the material in contact with the thermocouples must be a good electrical conductor. Moreover, the thermal diffusivity of aluminium ($k_{al} = 237$ W/m/K, $\rho_{al} = 2700$ kg/m^3 and $C_{al} = 900$ J/kg/K, $a_{al} \approx 10^{-4}$ m^2/s) is noticeably greater than that of the materials commonly studied and very thin slabs could be used ($e \approx 0.5$ mm). Thus, it also permits to reduce the delay in the heat diffusion due to the presence of the slabs.

As regards the course of the FLASH measurement, it is exactly identical to classical measurements.

3. Identification of the thermal conductivity of the sample

We have seen that our modified method uses an original experimental apparatus whose shape and size are similar to the ones used for the classical FLASH method. Actually, the main innovation of our modified method concerns the identification procedure allowing to estimate the thermal conductivity of the material. Indeed, the identification method permit to take into account the disturbing influence of the sample container very faithfully. It is based on a least square fit method which uses the Gauss linearization procedure.

3.1. Gauss linearization method

The least square fit method used requires the plotting of the temperature measured at the center of the back side of the irradiated sample $T_{\exp}(t)$ and a numerical model allowing to compute the theoretical variations $T_{\text{num}}(t)$ of the same temperature for a given sample and for given experimental conditions.

The principle is to minimize the function F representing the sum of the quadratic discrepancy between the experimental and theoretical variations of the temperature:

$$F = \sum_{i=1}^{N} \left[T_{\exp}(t_i) - T_{\text{num}}(t_i)\right]^2 \tag{1}$$

In the next section, we will see that the parameters influencing the evolution of the temperature calculated by our theoretical model are the shape and dimensions of the sample, the composition of the sample, the physical properties of the different pieces composing the sample and the experimental conditions. All these parameters are known except the thermal diffusivity of the sample a_{sam} and the convection coefficient h prevailing on the external surfaces of the container. Moreover, if the density ρ_{sam} and specific heat C_{sam} of the sample are known, the thermal conductivity k_{sam} is the only unknown parameter. The exchange coefficient h is assumed identical for all the surfaces. Thus, $T_{\text{num}}(t)$ and consequently F only depend on these two parameters:

$$F = F(k_{\text{sam}}, h) = \sum_{i=1}^{N} \left[T_{\exp}(t_i) - T_{\text{num}}(t_i, k_{\text{sam}}, h)\right]^2 \tag{2}$$

In order to minimize F, the parameters k_{sam} and h should satisfy the relations:

$$\begin{aligned}
&\frac{\partial F}{\partial k_{\text{sam}}} = \frac{\partial}{\partial k_{\text{sam}}}\left[\sum_{i=1}^{N}\left(T_{\exp}(t_i) - T_{\text{num}}(t_i)\right)^2\right] = 0\\
&\sum_{i=1}^{N}\left[\left(T_{\exp}(t_i) - T_{\text{num}}(t_i)\right)\frac{\partial T_{\text{num}}(t_i)}{\partial k_{\text{sam}}}\right] = 0\\
&\Longleftrightarrow\\
&\frac{\partial F}{\partial h} = \frac{\partial}{\partial h}\left[\sum_{i=1}^{N}\left(T_{\exp}(t_i) - T_{\text{num}}(t_i)\right)^2\right] = 0\\
&\sum_{i=1}^{N}\left[\left(T_{\exp}(t_i) - T_{\text{num}}(t_i)\right)\frac{\partial T_{\text{num}}(t_i)}{\partial h}\right] = 0
\end{aligned} \tag{3}$$

The partial derivatives $\partial T_{\text{num}}(t_i)/\partial h$ and $\partial T_{\text{num}}(t_i)/\partial k_{\text{sam}}$ are called the sensibility coefficients and represent the rate of variation of the temperature at the center of the back side at the time t_i due to a variation of the parameters h and k_{sam}.

In order to solve this system of non-linear equations, we use the iterative method of Gauss starting from initial values k^0_{sam} and h^0. At each iteration level l, the following system of equations is solved:

$$\begin{aligned}
&\sum_{i=1}^{N}\left[\left(T_{\exp}(t_i) - \left(T_{\text{num}}(t_i)\right)^l\right)\left(\frac{\partial T_{\text{num}}(t_i)}{\partial k_{\text{sam}}}\right)^l\right] = 0\\
&\sum_{i=1}^{N}\left[\left(T_{\exp}(t_i) - \left(T_{\text{num}}(t_i)\right)^l\right)\left(\frac{\partial T_{\text{num}}(t_i)}{\partial h}\right)^l\right] = 0
\end{aligned} \tag{4}$$

Moreover, the value $(T_{\text{num}}(t_i))^l$ at the iteration level l can be approximated from the values at the iteration level $l-1$ by the following relation:

$$\begin{aligned}
&\left(T_{\text{num}}\left(t_i, k^{l-1}_{\text{sam}} + \Delta k^{l-1}_{\text{sam}}, h^{l-1} + \Delta h^{l-1}\right)\right)^l\\
&\quad = \left(T_{\text{num}}\left(t_i, k^{l-1}_{\text{sam}}, h^{l-1}\right)\right)^{l-1} + \left(\frac{\partial T_{\text{num}}(t_i)}{\partial k_{\text{sam}}}\right)^{l-1}\Delta k^{l-1}_{\text{sam}}\\
&\qquad + \left(\frac{\partial T_{\text{num}}(t_i)}{\partial h}\right)^{l-1}\Delta h^{l-1}
\end{aligned} \tag{5}$$

We finally have the following matrix system, where the superscript l refer to the entire matrixes in order to lighten the formula:

$$\begin{aligned}
&\begin{bmatrix}
\sum_{i=1}^{N}\left(\frac{\partial T_{\text{num}}(t_i)}{\partial k_{\text{sam}}}\right)^2 & \sum_{i=1}^{N}\left(\frac{\partial T_{\text{num}}(t_i)}{\partial k_{\text{sam}}}\right)\left(\frac{\partial T_{\text{num}}(t_i)}{\partial h}\right)\\
\sum_{i=1}^{N}\left(\frac{\partial T_{\text{num}}(t_i)}{\partial k_{\text{sam}}}\right)\left(\frac{\partial T_{\text{num}}(t_i)}{\partial h}\right) & \sum_{i=1}^{N}\left(\frac{\partial T_{\text{num}}(t_i)}{\partial h}\right)^2
\end{bmatrix}^l
\begin{bmatrix}\Delta k_{\text{sam}}\\ \Delta h\end{bmatrix}^l\\
&\quad = \begin{bmatrix}
\sum_{i=1}^{N}\left(\left(T_{\exp}(t_i) - T_{\text{num}}(t_i)\right)\frac{\partial T_{\text{num}}(t_i)}{\partial k_{\text{sam}}}\right)\\
\sum_{i=1}^{N}\left(\left(T_{\exp}(t_i) - T_{\text{num}}(t_i)\right)\frac{\partial T_{\text{num}}(t_i)}{\partial h}\right)
\end{bmatrix}^l
\end{aligned} \tag{6}$$

This system is solved successively for each iteration level l to calculate the values $k^{l+1}_{\text{sam}} = k^l_{\text{sam}} + \Delta k^l_{\text{sam}}$ and $h^{l+1} = h^l + \Delta h^l$ until the ratios $\Delta k^l_{\text{sam}}/k^l_{\text{sam}}$ and $\Delta h^l/h^l$ are lower than a convergence criterion.

3.2. Numerical model of heat transfer in the complex sample

The identification method described in the previous section requires a theoretical model reproducing as faithfully as possible the transient thermal heat transfer in the sample. Indeed, the accuracy of the thermal conductivity identified is strongly dependent on the adequacy of the model. This model should simulate the thermal transport in the complex structure of the sample container. Consequently, it must take into account the shape and dimensions of the sample container, the properties of each part composing the sample and the experimental conditions in which the measurement was applied.

3.2.1. Governing equations

The thermal balance in a material submitted to a transient heat transfer is governed by the energy equation relating the variation of the local temperature to the heat flux divergence:

$$\rho C\frac{\partial T}{\partial t} = -\Delta(\vec{q}_t) = -\left[\Delta(\vec{q}_r) + \Delta(\vec{q}_c) + \Delta(\vec{q}_{\text{conv}})\right] \tag{7}$$

In our case, the medium in which the heat transfer occurs (sample container) is composed of several parts (aluminium slabs, Plexiglas circlet and sample) with different thermophysical properties. However, all the materials composing the sample container could be considered as opaque in the I.R. and thus, the radiative heat transfer can be neglected. As regards the convective heat transfer in the case of liquid materials, if we compute, for example, the Rayleigh number in water for a maximum temperature rise of the front side equal to 0.2 K, we find $Ra \approx 500$. But, for a Rayleigh number less than 1400, one can consider that natural convection phenomenon are negligible. Consequently, the convective heat transfer could also be neglected in all the part of the sample. Thus, the heat transfer is purely conductive in the entire sample.

In order to simplify the resolution of the energy equation, one can remark that our sample container is axisymmetric and thus, the temperature distribution in the sample is a function of the radial, axial and polar coordinates r, z and φ. If we also assume that the physical properties of the materials composing the sample are homogeneous and isotropic, the temperature field is independent of the polar angle φ and the energy equation in each part of the sample reduces to:

$$\rho C\frac{\partial T(r,z,t)}{\partial t} = k\frac{\partial^2 T}{\partial r^2} + \frac{1}{r}k\frac{\partial T}{\partial r} + k\frac{\partial^2 T}{\partial z^2} \tag{8}$$

As regards the time boundary conditions, the medium is at a uniform temperature before the beginning of the heating. This temperature is the external temperature and then:

$$\forall r \text{ and } z, \quad T(r,z,0) = T_{\text{ext}} \tag{9}$$

During the pulse irradiation of the sample by the FLASH (duration τ), the front face of the sample collects a heating power per surface unit $\dot{Q}$. In our numerical model, we assume that this radiative energy is entirely absorbed after a small penetration length χ and that the heat is uniformly generated along its path in the aluminium slab. Thus, the heat generation could be treated as an internal heat source. If we assume that the heating power is uniform on all the surface, we have, for the region $0 < z < \chi$; $0 < r < R_{\max}$:

$$\rho_{\text{al}} C_{\text{al}}\frac{\partial T_{\text{al}}(r,z,t)}{\partial t}\chi = \dot{Q} \quad \text{for } 0 < t < \tau \tag{10}$$

Given that the sample is composed of several parts with different thermophysical properties, several boundary conditions also occur at the interface between the different parts:

– At the horizontal interfaces between the aluminium slabs and the sample ($z = e$ and $z = L - e$ with $r < R_{\text{plex}}$), if we neglect the thermal resistance, the conductive heat fluxes balance leads to:

$$\left(k_{\text{al}}\frac{\partial T_{\text{al}}}{\partial z}\right)_{z=e^-} = \left(k_{\text{sam}}\frac{\partial T_{\text{sam}}}{\partial z}\right)_{z=e^+} \quad \text{and}$$
$$\left(k_{\text{al}}\frac{\partial T_{\text{al}}}{\partial z}\right)_{z=(L-e)^+} = \left(k_{\text{sam}}\frac{\partial T_{\text{sam}}}{\partial z}\right)_{z=(L-e)^-} \tag{11}$$

– Similarly, at the horizontal interfaces between the aluminium slabs and the Plexiglas ($z = e$ and $z = L - e$ with $R_{\max} > r > R_{\text{plex}}$), we have:

$$\left(k_{\text{al}}\frac{\partial T_{\text{al}}}{\partial z}\right)_{z=e^-} = \left(k_{\text{plex}}\frac{\partial T_{\text{plex}}}{\partial z}\right)_{z=e^+} \quad \text{and}$$
$$\left(k_{\text{al}}\frac{\partial T_{\text{al}}}{\partial z}\right)_{z=(L-e)^+} = \left(k_{\text{plex}}\frac{\partial T_{\text{plex}}}{\partial z}\right)_{z=(L-e)^-} \tag{12}$$

– At the vertical interface between the sample and the side of the container ($e < z < L - e$ and $r = R_{\text{plex}}$), we have:

$$k_{\text{plex}}\frac{\partial T_{\text{plex}}}{\partial r} = k_{\text{sam}}\frac{\partial T_{\text{sam}}}{\partial r} \tag{13}$$

The external surfaces of the sample are also submitted to thermal boundary conditions due to the convective and radiative heat transfer with the external environment. The rate of heat exchange by radiation is equal to $\varepsilon\sigma(T_s^4 - T_{\text{ext}}^4)$. So, for a relatively small difference $T_s - T_{\text{ext}}$, we have: $\varepsilon\sigma(T_s^4 - T_{\text{ext}}^4) \approx \varepsilon\sigma T_s^3(T_s - T_{\text{ext}})$. Consequently, the total heat transfer between the external surfaces could be summarized in a unique coefficient h, which takes into account the convective and radiative exchanges: $h = h_{\text{conv}} + \varepsilon\sigma T_s^3$. If we also assume that the convection coefficients h_{conv} and the temperatures T_s on the horizontal and vertical surfaces are identical, the thermal boundary conditions on these surfaces are the same and reduce to:

$$k_{\text{plex}}\left(\frac{\partial T_{\text{plex}}}{\partial r}\right) = -h(T_{\text{plex}} - T_{\text{ext}}) \tag{14}$$

for the surface defined by $r = R_{\max}$, $e < z < L - e$

$$k_{\text{al}}\left(\frac{\partial T_{\text{al}}}{\partial r}\right) = -h(T_{\text{al}} - T_{\text{ext}}) \tag{15}$$

for the surfaces defined by $r = R_{\max}$; $0 < z < e$ and $r = R_{\max}$; $L - e < z < L$

$$k_{\text{al}}\left(\frac{\partial T_{\text{al}}}{\partial z}\right)_{z=0} = h(T_{\text{al}} - T_{\text{ext}})_{z=0} \quad \text{and}$$
$$k_{\text{al}}\left(\frac{\partial T_{\text{al}}}{\partial z}\right)_{z=L} = -h(T_{\text{al}} - T_{\text{ext}})_{z=L} \tag{16}$$

for the surfaces defined by $z = 0$, $0 < r < R_{\max}$ and $z = L$, $0 < r < R_{\max}$, respectively.

3.2.2. Numerical resolution of the transient heat transfer

In order to solve the energy equation (2) and to calculate numerically the variation of the temperature field at the backside of the sample, we use an explicit time marching technique.

At each time step, the resolution of the energy equation permits to compute the new temperature distribution from the temperature profiles at the previous time step. To solve this equation we use spatial discretizations dividing the entire sample in $nR \times nZ$ elementary volumes. The discretizations along

the z-axis and r-axis differ according to the zone considered. Four different zones are considered:

- The aluminium slab at the front side of the sample delimited by $0 < z < e$ ($j = 1, nZ_{al}$) and $0 < r < R_{max}$ ($i = 1, nR$) for which $\Delta r_i = R_{plex}/(nR - nR_{plex})$ for $i = 1, nR - nR_{plex}$; $\Delta r_i = (R_{max} - R_{plex})/nR_{plex}$ for $i = nR - nR_{plex}, nR$ and $\Delta z_j = e/nZ_{al}\ \forall j$.
- The aluminium slab at the back side of the sample delimited by $L - e < z < L$ ($j = nZ - nZ_{al}, nZ$) and $0 < r < R_{max}$ ($i = 1, nR$) for which $\Delta r_i = R_{plex}/(nR - nR_{plex})$ for $i = 1, nR - nR_{plex}$; $\Delta r_i = (R_{max} - R_{plex})/nR_{plex}$ for $i = nR - nR_{plex}, nR$ and $\Delta z_j = e/nZ_{al}\ \forall j$.
- The Plexiglas circlet delimited by $e < z < L - e$ ($j = nZ_{al} + 1, nZ - nZ_{al}$) and $R_{plex} < r < R_{max}$ ($i = nR - nR_{plex}, nR$) for which $\Delta r_i = (R_{max} - R_{plex})/nR_{plex}$ and $\Delta z_j = (L - 2e)/(nZ - 2nZ_{al})\ \forall j$.
- The sample delimited by $e < z < L - e$ ($j = nZ_{al} + 1, nZ - nZ_{al}$) and $0 < r < R_{plex}$ ($i = 1, nR - nR_{plex}$) for which $\Delta r_i = R_{plex}/(nR - nR_{plex})$ and $\Delta z_j = (L - 2e)/(nZ - 2nZ_{al})\ \forall j$.

At the center and on the radial faces of each elementary volume (i, j), there is a node. The numerical resolution computes the temperature at the center (noted $T_{i,j}$) and on the boundary (noted $T_{i\pm1/2,j}$) of each volume.

For the nodes (i, j) belonging to a zone k, which have no boundary with any node of another region, if we express the energy equation (4) in a discretized form using Eq. (4), we could express the new temperature (time $t + 1$) from the temperature profile at previous time step (time t):

$$T_{i,j}^{t+1} = T_{i,j}^{t} + \frac{\Delta t}{\rho_k C_k}\left[4k_k\frac{T_{i+1/2,j}^{t} - 2T_{i,j}^{t} + T_{i-1/2,j}^{t}}{\Delta r_i^2} + \frac{k_k}{r_i}\left(\frac{T_{i+1/2,j}^{t} - T_{i-1/2,j}^{t}}{\Delta r_i}\right) + k_k\frac{T_{i,j+1}^{t} - 2T_{i,j}^{t} + T_{i,j-1}^{t}}{\Delta z_j^2}\right] \quad (17)$$

Similar relations could be found easily for the nodes placed on the boundary of the elementary volumes.

For the nodes located at the front side of the top aluminium slab ($j = 1$ and $i = 1, nR$), if we take into account the boundary conditions (Eqs. (10) and (16)) assuming that the energy is entirely absorbed in the first node along the z-axis, we can apply an energy balance and we have:

$$T_{i,j}^{t+1} = T_{i,j}^{t} + \frac{\Delta t}{\rho_{al} C_{al} V_{i,j}}\left[\dot{Q}S_{i,j} - hS_{i,j}\left(T_{i,j}^{t} - T_{ext}\right) + k_{al}S_{i,j}\frac{T_{i,j+1}^{t} - T_{i,j}^{t}}{\Delta z_j} + 2\pi r_{i-1/2}\Delta z(j)k_{al}\frac{T_{i-1/2,j}^{t} - T_{i,j}^{t}}{\Delta r_i/2} + 2\pi r_{i+1/2}\Delta z(j)k_{al}\frac{T_{i+1/2,j}^{t} - T_{i,j}^{t}}{\Delta r_i/2}\right] \quad (18)$$

when $0 < t < \tau$ and

$$T_{i,j}^{t+1} = T_{i,j}^{t} + \frac{\Delta t}{\rho_{al} C_{al} V_{i,j}}\left[-hS_{i,j}\left(T_{i,j}^{t} - T_{ext}\right) + k_{al}S_{i,j}\frac{T_{i,j+1}^{t} - T_{i,j}^{t}}{\Delta z_j} + 2\pi r_{i-1/2}\Delta z(j)k_{al}\frac{T_{i-1/2,j}^{t} - T_{i,j}^{t}}{\Delta r_i/2} + 2\pi r_{i+1/2}\Delta z(j)k_{al}\frac{T_{i+1/2,j}^{t} - T_{i,j}^{t}}{\Delta r_i/2}\right] \quad (19)$$

when $t > \tau$.

For the nodes located at the backside of the bottom aluminium slab ($j = nZ$ and $i = 1, nR$), if we take into account the boundary condition (Eqs. (10) and (16)) and if we apply an energy balance, we have:

$$T_{i,j}^{t+1} = T_{i,j}^{t} + \frac{\Delta t}{\rho_{al} C_{al} V_{i,j}}\left[-hS_{i,j}\left(T_{i,j}^{t} - T_{ext}\right) + k_{al}S_{i,j}\frac{T_{i,j-1}^{t} - T_{i,j}^{t}}{\Delta z_j} + 2\pi r_{i-1/2}\Delta z(j)k_{al}\frac{T_{i-1/2,j}^{t} - T_{i,j}^{t}}{\Delta r_i/2} + 2\pi r_{i+1/2}\Delta z(j)k_{al}\frac{T_{i+1/2,j}^{t} - T_{i,j}^{t}}{\Delta r_i/2}\right] \quad (20)$$

Similarly, for the nodes located at the interface between the Plexiglas circlet and the air ($i = nR$ and $j = nZ_{al} + 1, nZ - nZ_{al}$), the boundary condition (Eq. (14)) leads to:

$$T_{i,j}^{t+1} = T_{i,j}^{t} + \frac{\Delta t}{\rho_{plex} C_{plex} V_{i,j}}\left[-hS_{i,j}\left(T_{i,j}^{t} - T_{ext}\right) + k_{plex}S_{i,j}\frac{T_{i,j+1}^{t} - T_{i,j}^{t}}{\Delta z_j} + k_{plex}S_{i,j}\frac{T_{i,j-1}^{t} - T_{i,j}^{t}}{\Delta z_j} + 2\pi r_{i-1/2}\Delta z(j)k_{plex}\frac{T_{i-1/2,j}^{t} - T_{i,j}^{t}}{\Delta r_i/2}\right] \quad (21)$$

Similar relations can be obtained for the nodes located at the interface between Plexiglas-sample (Eq. (13)), aluminium-sample (Eq. (11)) and Plexiglas-aluminium (Eq. (12)).

3.2.3. Validation of the numerical model

The numerical model developed for the identification of the thermal conductivity of the sample takes into account the conductive heat transfer in each part of the sample container. Unfortunately, at the moment, very few results on the modeling of the transient conductive heat transfer in composite materials with complex geometries are available in the literature. Moreover, most of these works concern thermal and time boundary conditions, which are noticeably different from the ones encountered during the FLASH measurement. Consequently, the validation of our model could only be conducted by considering the case of the transient heat transfer in a homogeneous material.

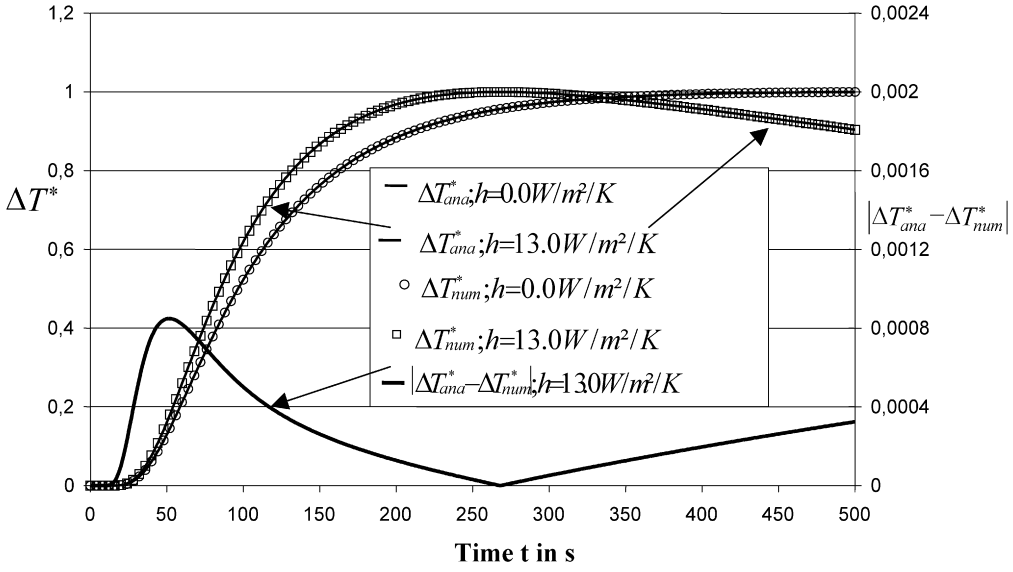

Fig. 2. Comparison of the evolution of the dimensionless temperature calculated analytically and numerically for a 10 mm slab of water ($k = 0.6$ W/m/K; $\rho = 100$ kg/m^3; $C = 4180$ J/kg/K) with $h = 0.0$ W/m^2/K and $h = 13.0$ W/m^2/K.

Then, for a 1-D heat transfer in an homogeneous slab uniformly irradiated by a Dirac time distribution function and submitted to convective heat losses on its front and back sides, the dimensionless temperature rise at the back side is given by:

$$\Delta T^*_{\text{ana}} = \frac{Q}{\rho C L} Z(t^*, H) \quad \text{with}$$

$$Z(t^*, H) = \sum_{n=0}^{\infty} \frac{2u_n^2(u_n^2 + H^2)}{u_n^2 + H^2 + 2H} \frac{\cos(u_n)}{u_n^2 - H^2} \exp\left(-u_n^2 t^*\right) \tag{22}$$

where $H = hL/k$ is the Biot number shared by both sides and $t^* = (k/\rho C L^2)t$ the Fourier number of the sample and u_n the solutions of the transcendent equation:

$$\sin(u)\left[u^2 - H^2\right] = u\cos(u)2H \tag{23}$$

We computed the variations of ΔT^*_{ana} in the fictive case where a 10 mm slab of water ($L = 0.01$ m, $k = 0.6$ W/m/K; $\rho = 1000$ kg/m^3; $C = 4180$ J/kg/K) was irradiated by a Dirac time distribution function with $Q = 1$ J/m^2. The heat exchange coefficient h was set to 0 W/m^2/K or 13.0 W/m^2/K. In practice, the summation required for the computation of $Z(t^*, H)$ is conducted for $n = 0$, 100 instead of $n = 0$, ∞. We checked that the relative error due to this curtailment is lower than 0.1%. We compared the evolutions of the dimensionless temperature obtained analytically with the results of our model for the time range $0 \rightarrow 500$ s. The dimensionless temperature T^* is defined by:

$$\Delta T^* = \frac{T - T_{\text{ext}}}{T_{\max} - T_{\text{ext}}} \quad \text{where}$$

$T_{\max}$ is the maximum temperature reached during the heating

Given that we had to simulate the 1-D heat transfer in a homogeneous medium, we set $R_{\max} = 10$ m and $k_{\text{plex}} = k_{\text{al}} = k_{\text{water}} = 0.6$ W/m/K for the numerical computation. Moreover, in order to simulate a Dirac excitation, the duration of the FLASH excitation was set to a very small value: $\tau = 100$ ms. The other parameters used are: $nR = 3$, $nZ = 40$, $R_{\text{plex}} = 7$ m, $nR_{\text{plex}} = 1$, $e = 0.25$ mm, $nZ_{\text{al}} = 1$.

The comparisons are illustrated in Fig. 2 for both cases ($h = 0.0$ and $h = 13.0$ W/m^2/K). We also illustrate, in this figure, the difference $|\Delta T^*_{\text{ana}} - \Delta T^*_{\text{num}}|$ between the analytical and numerical computations in the latter case.

One can observe that the evolution of the temperature predicted by our numerical model is in close agreement with the analytical solution for the two cases considered. The temperature difference $|\Delta T^*_{\text{ana}} - \Delta T^*_{\text{num}}|$ is always lower than 0.001. Consequently, we could consider that our numerical model gives accurate simulations of the 1-D heat transfer in a homogeneous medium.

4. Estimation of the measurement uncertainties

In order to validate our method of measurement, we carried out an exhaustive review of the parameter, which are likely to cause errors on the evaluation of the thermal diffusivity. We divided these parameters in three different categories: the parameters related to the morphology and properties of the container, the parameters related to the deviation from the hypothesis of the model and the parameters related to the accuracy of the measuring apparatus.

4.1. Errors due to the uncertainties on the dimensions and the thermophysical properties of the container

Our identification method is based on an accurate modeling of the thermal heat transfer in the real sample containers. The dimensions of these containers and the properties of the different materials constituting the container are measured as accurately as possible. However, there subsist some uncertainties on these values, which could influence the thermal diffusivity identified. That is the reason why, we have conducted an evaluation

Table 1
Values of $\partial k_{\text{sam}}/\partial p_i$ for the six parameters characterizing the sample container

Parameter	a_{plex}	a_{Al}	L	e	$R_{\max} - R_{\text{plex}}$	$R_{\max}$
$\partial k_{\text{sam}}/\partial p_i$ in % per %	0.065	0.0043	2.25	0.086	0.041	0.055

of the errors that might be caused by a bad evaluation of these parameters. The different parameters are:

- the thermal diffusivity a_{plex} of Plexiglas;
- the thermal diffusivity a_{al} of aluminium;
- the height of the sample L;
- the thickness of the aluminium caps e;
- the thickness of the Plexiglas circlet $R_{\max} - R_{\text{plex}}$;
- the radius of the sample container $R_{\max}$.

For each parameter p_i, we computed numerically the variation $\frac{\partial k_{\text{sam}}}{\partial p_i}(p_i^0)$, which represents the influence, on the thermal conductivity, identified k_{liq}, of an error ∂p_i on the parameter p_i around the nominal value p_i^0. We have:

$$\frac{\partial k_{\text{sam}}}{\partial p_i}\left(p_i^0\right) \approx \frac{k_{\text{sam}}(p_i^0 + \Delta p_i) - k_{\text{sam}}(p_i^0)}{\Delta p_i} \tag{24}$$

where $k_{\text{sam}}(p_i^0 + \Delta p_i)$ is the thermal conductivity identified from the thermogram obtained with $p_i = p_i^0 + \Delta p_i$, all the other parameters remaining unchanged and $k_{\text{sam}}(p_i^0) = k_c$ is the thermal conductivity of the sample used for the computation. $\frac{\partial k_{\text{sam}}}{\partial p_i}(p_i^0)$ could be expressed in % per %. We conducted the computations of $\frac{\partial k_{\text{sam}}}{\partial p_i}(p_i^0)$ for a sample container filled with water ($k_c = 0.6$ W/m/K, $\rho = 1000$ kg/m^3, $C = 4180$ J/kg/K), using the nominal values p_i^0 of L, $R_{\max}$, R_{plex}, e, a_{plex} and a_{Al} indicated in Section 3.2.3. We also assume $h = 13.0$ W/m^2/K. Table 1 summarizes the results obtained.

One can notice that the thickness of the sample is, by far, most influencing parameter.

From these values, we can evaluate the uncertainties $(\Delta k_{\text{sam}})_i$ on the value of k_{sam} identified due to an error Δp_i on the estimation of the parameter p_i. We have:

$$\frac{(\Delta k_{\text{sam}})_i}{k_{\text{sam}}} = \frac{\partial k_{\text{sam}}}{\partial p_i}\frac{\Delta p_i}{p_i} \tag{25}$$

The maximal relative errors on the six parameters characterizing the sample container have been evaluated:

- According to the literature data, the relative uncertainties on the Plexiglas and aluminium thermal diffusivities are: $\Delta a_{\text{plex}} = 2\%$; $\Delta a_{\text{al}} = 2\%$;
- The thickness L of each sample container is measured using a digital caliper. The uncertainty provided by this apparatus is 0.05 mm. The container used has a thickness of approximately 10 mm. If we assume that the container has a strictly constant thickness, we then have: $\Delta L/L = 0.05$ mm$/10$ mm $= 0.5\%$;
- Similarly the relative uncertainty on the thickness of aluminium slab is $\Delta e = 0.05$ mm$/0.5$ mm $= 10\%$;
- Moreover, $\Delta(R_{\max} - R_{\text{plex}}) = 0.05$ mm$/1.7$ mm $= 3\%$;
- Similarly, $\Delta R_{\max} = 0.05$ mm$/15$ mm $= 0.33\%$.

If we add the contributions of each relative error on the relative uncertainty on the value of the diffusivity identified, we have a global error of approximately 2.5%.

4.2. Errors due to the deviation from the hypothesis of the model

The main assumptions made by the model concern the modes of heat transfer. Indeed, we neglected the radiative and convective contributions in the sample and considered that a purely conductive transfer occurs in a homogeneous material. We also assumed that the convective heat transfer coefficient is identical for each outside surfaces of the container.

As regards radiative heat transfer, the values of the imaginary part of the refractive index of water given in the literature, notably by Segelstein [27], clearly indicate that no infrared radiation can propagate in this liquid. The absorption coefficient is greater than 1000 m^{-1} in the wavelength range [2–50 μm] which corresponds to a radiant conductivity (Rosseland approximation) lower than 0.0001 W/m/K at ambient temperature. Consequently we can consider that this assumption does not lead to any error when measurements are made on materials containing a significant proportion of water. Moreover, most liquids can be assumed opaque to Infrared radiation and thus, the assumption of no radiative heat transfer is fully justified except in some outstanding cases of transparent liquids.

Similarly, we have seen in Section 3.2.1 that the convective phenomenon in liquids can also be neglected in our FLASH measurement since the temperature rise is very small and since the heated boundary is the top slab. Therefore, we will consider that this assumption does not lead to any uncertainty. On the other hand, for the convective heat transfer between the container and the environment, we assumed, for simplicity purpose, that the exchange coefficient h is the same for all the exterior surfaces. In practice, noticeable differences can be found between the two horizontal and the vertical boundaries. For example, it is obvious that the convective exchange between the top surface and the environment is more important than for the bottom side. The use of some empirical correlations of the literature [28] for horizontal plane slabs oriented upwards or downwards or for vertical cylinder shows that the mean exchange coefficients are similar for the lateral and top boundaries and approximately half these values for the bottom boundary. Consequently, we have been able to evaluate the uncertainty by computing the temperature evolution with an exchange coefficient h_1 equal for the lateral and top boundaries and a coefficient $h_2 = h_1/2$ for the bottom boundary. Thereafter, we identified the thermal diffusivity, which would

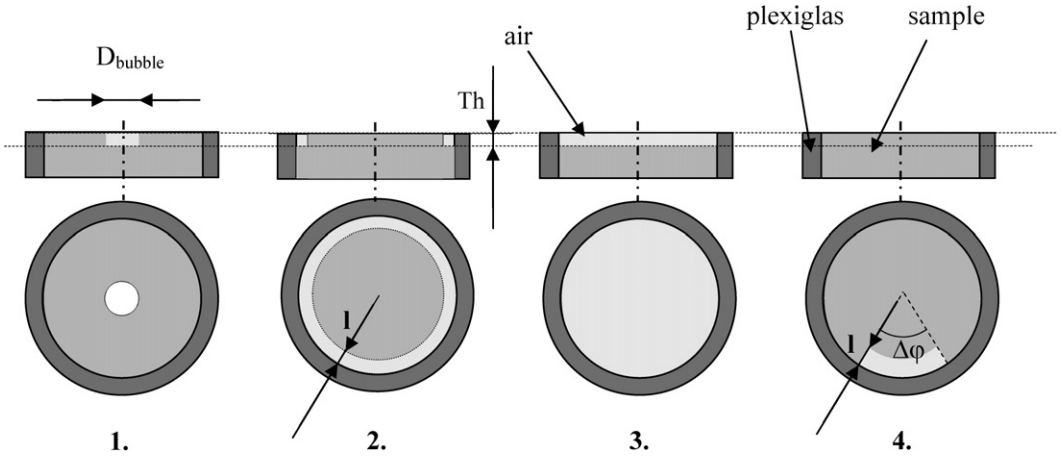

Fig. 3. Cutting-view and above view illustrating the four configurations simulated to estimate the influence of the presence of the air bubble.

be identified using the model assuming a unique exchange coefficient h on all the exterior surfaces. The deviation from the exact thermal diffusivity of the sample gives a good estimation of the error. We conducted the computations for water in the sample container of Section 3.2.3 and with $h_1 = 13.0\ \mathrm{W/m^2/K}$ and $h_2 = 6.5\ \mathrm{W/m^2/K}$. In these conditions, the relative difference between the thermal diffusivity identified and the thermal diffusivity of water used for the computation is only 0.2%. Moreover, we only considered here the convective surface exchange. In practice, a significant part of the heat losses at the surfaces is due to thermal radiation. We have seen that the radiative exchange coefficient varies in T^3. Since the temperature of each surfaces are sensibly equal (very weak temperature rise), the coefficients of radiative exchange of the three surfaces are almost identical and thus, the differences in global surface exchange coefficients ($h = h_{\mathrm{conv}} + \varepsilon\sigma T_s^3$) between the surfaces is surely lower than that considered in our calculations. Consequently, a relative uncertainty of 0.2% can be retained for the assumption of constant exchange coefficient.

Finally, one of the main difficulties of our method is to be able to obtain a homogeneous sample phase, especially in the case of liquid materials. Indeed, it is difficult to fill the sample container uniquely with the liquid tested. Practically, a very small quantity of gas could subsist after the introduction of the liquid or could enter the container due to air tightness defaults of the container cap. Evaporation in highly volatile liquids or air desorption could also occur. In these cases, the gas phase is gathered in a small unique bubble located at the top of the Plexiglas cylinder. Such bubbles are sometimes observed even when a meticulous filling of the container is conducted. In practice, due to the gravity forces, the bubble is always located at the top of the sample volume near the border of the Plexiglas cylinder. The order of magnitude of the characteristic size of the bubbles is approximately 1 mm (when it is present). So, if we assume that the bubbles are spherical with a radius $R = 1$ mm the volume fraction of air remains lower than 1% (0.7% exactly).

The presence of the bubbles may cause an error in the estimation of the thermal conductivity as the thermal heat transfer is noticeably reduced locally. That is the reason why a perfect filling of the container should be conducted ideally. However, in order to estimate the errors, which would be caused by the presence of air, we carried out the calculation of the theoretical evolution of the dimensionless temperature at the backside of the sample container when an air bubble of various shapes and dimensions is present. Thereafter, we have introduced these theoretical thermograms in the identification procedure so as to determine the thermal diffusivity of the homogeneous material, which would best fit the thermal behavior. The error caused by the presence of air could then be estimated by the difference between the real thermal diffusivity of the sample and the diffusivity identified. The computations have been conducted with the thermal properties of water. We have simulated four different repartitions of the air illustrated in Fig. 3:

1. A cylindrical air bubble with diameter $D_{\mathrm{bubble}} = 5.9$ mm and height $Th = 3$ mm located at the bottom center of the top aluminium slab (configuration 1, air%: 1.7).
2. An air circlet of $l = 1.5$ mm in thickness and height $Th = 0.62$ mm located at the periphery of the sample, at the bottom of the top aluminium slab near the Plexiglas circlet (configuration 2, air%: 1.6).
3. A complete slab of air of height $Th = 0.21$ mm located just below the top aluminium slab (configuration 3, air%: 1.25).
4. An air bubble located in a section of the above slice (see Fig. 3) with $\Delta\varphi = \pi/3$, $Th = 3$ mm and $l = 0.15$ mm (configuration 4(a), air%: 1.2) or $\Delta\varphi = \pi/6$, $Th = 3$ mm and $l = 0.3$ mm (configuration 4(b), air%: 1.15).

Configurations 1, 2 and 3 could be simulated by simply replacing the thermal properties of water by that of air for the discretized nodes concerned. On the other hand, in configuration 4(a) and 4(b), the thermal problem is no more 2-D axisymmetric as the temperature distribution also depend on the polar angle φ. The energy equation becomes:

$$\rho C\frac{\partial T(r,z,\varphi,t)}{\partial t} = k\frac{\partial^2 T(r,z,\varphi,t)}{\partial r^2} + \frac{1}{r}k\frac{\partial T(r,z,\varphi,t)}{\partial r} + k\frac{\partial^2 T}{\partial z^2} + \frac{k}{r^2}\frac{\partial^2 T(r,z,\varphi,t)}{\partial \varphi^2} \tag{26}$$

Table 2
Illustration of the thermal conductivities and convective coefficients identified for the 5 different configurations of air bubble

Configuration number	Air volume fraction (%)	Convective coefficient h identified ($W\,m^{-2}\,K^{-1}$)	Thermal conductivity k identified ($W\,m^{-1}\,K^{-1}$)	Corresponding error (%)
1	1.7	13.2	0.5951	0.82
2	1.6	13.38	0.5969	0.52
3	1.25	14.92	0.5076	15.4
4(a)	1.22	13.08	0.5982	0.3
4(b)	1.15	13.08	0.5982	0.3

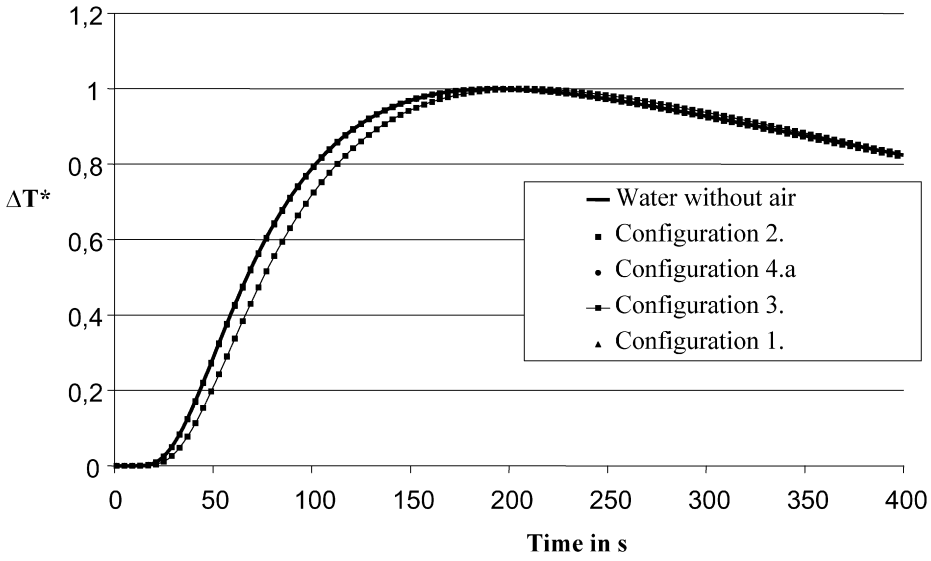

Fig. 4. Comparison of the theoretical thermograms obtained in the presence of air for the four different configurations.

Consequently, for these simulations, we have also discretized the sample volume along the polar angle φ in $n\varphi$ equal volumes covering an angle $\Delta\varphi = 2\pi/n\varphi$. The energy equation was solved in all the discretized volumes.

The numerical parameters are: $nR = 10$, $nZ = 40$ and $n\varphi = 12$. The physical properties of Plexiglas, aluminium and water and the dimensions of the sample container used are those illustrated in Section 3.2.3. For air, we used the following properties: $k_{air} = 0.026$ W/m/K, $\rho_{air} = 1.29$ kg/m^3, $C_{air} = 1006$ J/kg/K. Finally, we assumed a convective heat transfer $h = 13.0$ W/m^2/K.

The results of the identification for the five configurations are illustrated in Table 2. We also illustrate the thermograms obtained in the presence of water in the four different configurations and compare them with the ideal thermogram (absence of air) in Fig. 4.

One can remark that the influence of the presence of air strongly depends on the localization of the bubble. For example, if the air is arranged as a continuous slab located just below the aluminium cap (configuration 3), the conductive heat transfer is noticeably affected given that the air and the sample phase are associated in series. So, the heat is forced to travel across the air slab before reaching the backside. The slab of air acts as a thermal barrier. As a consequence, for a volume fraction of air of only 1.25%, a relative error of 15.4% is theoretically reached in this configuration.

For all the other configurations, the air does not form a continuous slab and thus the thermal heat transfer is practically not affected by the presence of air. The configuration for which the perturbation of the temperature at the center of the backside is the most important is configuration 1. This can be explained by the fact that the air is then located just above the place where the temperature is measured whereas, for the other configurations, the air is located on the border of the sample volume. However, the relative error due to the presence of air in configuration 1 is only 0.82% for a volume fraction of air of 1.7% which is much more important than the volume fraction actually encountered in practice.

In practice, configurations 4(a) or 4(b) are the best adapted to the case considered (bubble located at the top of the sample volume near the border of the Plexiglas cylinder). The relative error is then lower than 0.5%.

As a consequence, in the rest of the study, we will assume that the possible presence of a small amount of air results in a maximum relative uncertainty of 0.5% on the thermal conductivity identified.

4.3. Errors related to the accuracy of the measuring apparatus

The errors on the identification of the diffusivity caused by the uncertainties on the measured parameters are of two kinds: the uncertainties on the temperature scale and the uncertainty on the time scale.

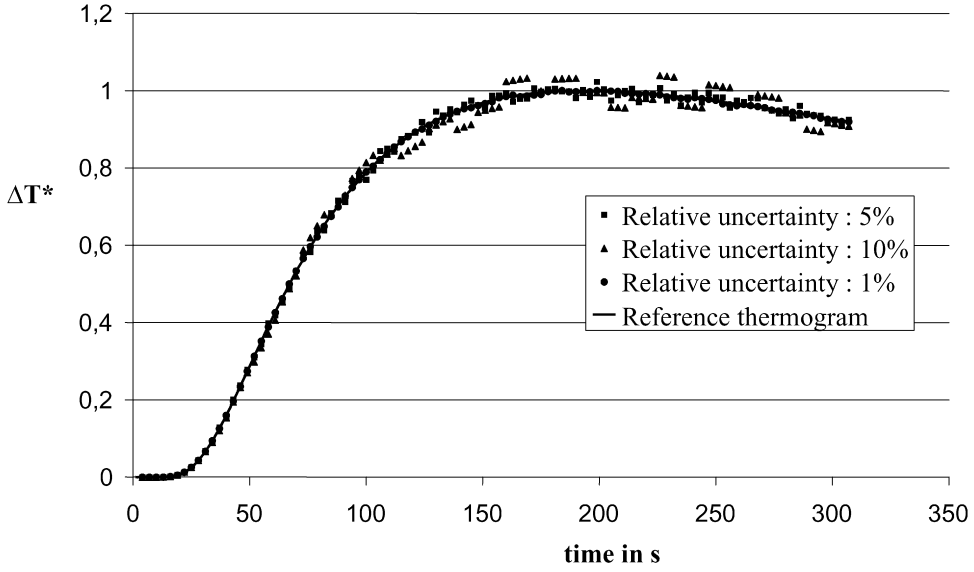

Fig. 5. Illustration of the noised thermograms for different relative uncertainties on the temperature measurement.

We have evaluated the influence of the errors on the temperature measured by computing the thermal diffusivity, which would be measured if a random relative error was made on each temperature measured on the thermogram. To do that, we simply modify the theoretical thermogram obtained with an usual sample container by randomly varying the values of each temperature recorded in the given uncertainty domain. By this manner, we obtain noised signals similar to the one illustrated in Fig. 5. The error on the estimation of the thermal diffusivity caused by the noise introduced can be estimated from the difference between the diffusivity identified in the presence of noise and the actual diffusivity of the material simulated. We carried out the computation for the sample container of Section 3.2.3 filled with water and assuming that $h = 13.0\ \mathrm{W/m^2/K}$. Three different relative uncertainties on the temperature scale were considered: 1%, 5% and 10%. The deviation of the thermal diffusivities identified from the thermal diffusivity of water used in the theoretical computation are respectively $+0.034\%$, $+0.21\%$ and -0.33%. One can notice that these deviations are extremely low even when a particularly important error is made on the measured temperature. In practice, for the apparatus used, a random deviation of 5% for the temperature recorded at the backside is an overestimating maximum. Consequently, we could consider that the uncertainty related to the measuring error on the temperature scale is 0.2%.

Similarly, concerning the uncertainty on the time scale of the thermogram, we have estimated its influence by identifying the thermal conductivity which would be identified if a relative error was made on the evaluation of time t. Contrary to the previous case, we assumed that this error is constant all along the measurement as it is due to an error on the estimation of the unreeling speed v of the recording paper. Then, we computed the parameter $\partial k_{\mathrm{sam}}/\partial t$ expressed in % per % representing the influence, on the thermal conductivity identified k_{sam}, of an error ∂t on the measured time. It has been calculated for the container described in Section 3.2.3 filled with water. In these conditions we have $\partial k_{\mathrm{sam}}/\partial t \approx 1.05\%$ per %. The error due to the relative uncertainty on the time recorded can be calculated by

$$\frac{(\Delta k_{\mathrm{sam}})_t}{k_{\mathrm{sam}}} = \frac{\partial k_{\mathrm{sam}}}{\partial v}\frac{\Delta t}{t} \tag{27}$$

For each measurement, the unreeling speed is controlled using a digital chronometer and the millimeter grading of the recording paper by measuring the time necessary for the paper to unroll a certain length. Thus, the relative uncertainty on the on the time scale is directly related to the relative uncertainty on the measurement of the unrolling duration. For measurements on water, the control of the time scale is conducted during approximately 200 s and the maximal error can be estimated $\Delta t \approx 1$ s and then $\Delta t/t \approx 0.5\%$.

Finally, we can consider that the uncertainty on the diffusivity identified due to the error on time scale is lower than 0.5%.

4.4. Estimation of the total uncertainty

By adding the different uncertainties evaluated in the previous sections, it appears that the total relative uncertainty on the measurement of the thermal diffusivity is lower than 4%.

5. Experimental validation

In order to validate the results of our method, we conducted several thermal diffusivity measurements on two different liquids (water and ethanol) and on a polyacrylamid gel commonly used for electrophoreses. The gel is composed of 10% of polyacrylamid with 90% of water. It has been used for thermal analysis, notably by Dittmar el al. [29] and its thermal properties have been investigated experimentally by Hirata et al. [30] for different polyacrylamid concentration and different temperature. As regards the thermal properties of water and ethanol, they are notably given in [31]. The properties of

Table 3
Thermal characteristics at 300 K of the liquids and gel used for the experimental validation of our method

Material	ρ in kg m^{-3}	C in J kg^{-1} K^{-1}	k in W m^{-1} K^{-1}	a in m^2 s^{-1}
Water [30]	9965	4179	0.611	1.47×10^{-7}
Ethanol [30]	795	2460	0.177	9.05×10^{-8}
Polyacrylamid gel [29]	1030	4000	0.593	1.44×10^{-7}

Table 4
Illustration of the average thermal conductivities measured with our modified FLASH method for different liquids

Material	Number of measurements	Average conductivity identified (W m^{-1} K^{-1})	Standard deviation (W m^{-1} K^{-1})	Average conductivity without corrections	Literature data k (W m^{-1} K^{-1}) at 25 °C
Water	9	0.619	0.0215	0.683	0.611
Ethanol	7	0.189	0.0216	0.192	0.177
Polyacrylamid gel	3	0.593	0.0176	0.662	0.593

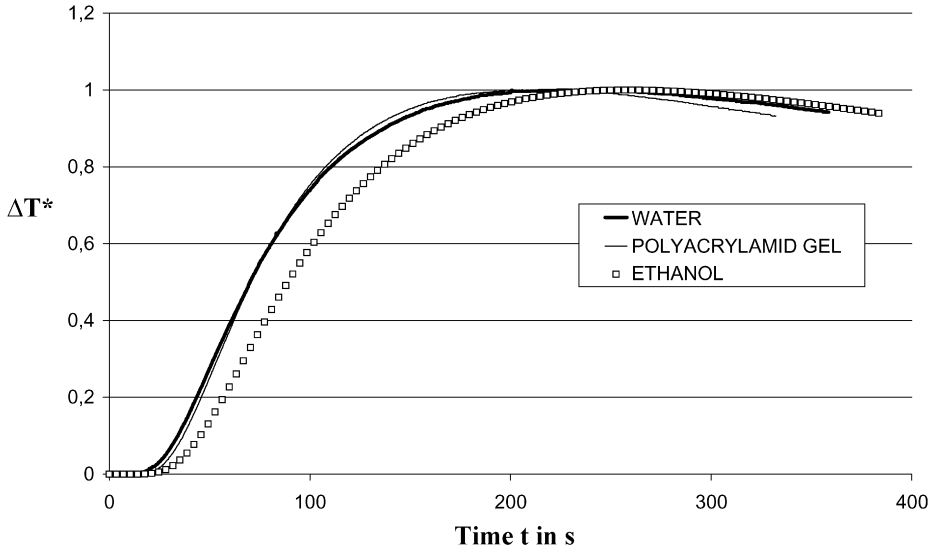

Fig. 6. Averaged thermograms obtained experimentally for the three different materials tested.

the three materials tested are regrouped in Table 3. For each material, we made a series of measurements of the thermal diffusivity and studied the distribution of the measured values. The results have been obtained at 300 K using a cylindrical receptacle with $R_{max} = 0.015$ m, $R_{plex} = 0.0133$ m, $e = 0.57$ mm and $L = 0.00965$ m. The results are summarized in Table 4 where we also indicate the number of measurements and the standard deviation of the measurements. In order to illustrate the disturbing influence of the sample container on the thermal heat transfer, we have also identified the thermal conductivity that would be measured if the sample container was neglected, i.e., if we consider that the sample was homogeneous and uniquely composed of the material tested. The corresponding thermal conductivity are reported in Table 4, and noted as "average conductivity without corrections". We also illustrate in Fig. 4 the thermograms averaged over all the measurements for the three materials tested.

One can remark a good agreement between our experimental measurements and the data indicated in the literature for the thermal conductivity of the three materials. The standard deviation of the conductivity measured is relatively low for water and the polyacrylamid gel but is more important for ethanol. The curves of Fig. 6 confirm that ethanol exhibits a smaller thermal diffusivity than the gel and water as the time required to reach the maximum temperature of the backside is more important.

One can also notice the strong influence of the receptacle on the thermal heat transfer for the measurements on water and polyacrylamid gel since the thermal conductivities identified with or without the corrections related to the influence of the container are noticeably different in these two cases. Then, it highlights the necessity to use a suitable identification procedure to obtain a consistent conductivity from the thermogram obtained experimentally. On the other hand, for measurements on ethanol, the thermal conductivities identified with or without the corrections related to the influence of the container are practically identical. This is due to the fact that the thermal diffusivity of ethanol and Plexiglas are close to each other. Then, the conductive heat transfer in the container is only weakly affected by the presence of Plexiglas circlet on the border.

We can conclude from the measurements on the three materials tested that our method proves to give coherent values of the thermal conductivity. It could be used successfully to estimate the thermal conductivity of other unknown liquids or pasty materials, which fulfill the assumptions made (opaque to thermal radiation, no convection).

6. Conclusion

We have developed an original method of measurement of the thermal conductivity of liquids or pasty materials. It is based on the well-known FLASH method that has been adapted to this kind of materials for which it is not possible to obtain homogeneous rigid samples with given and immoveable dimensions and shape.

The method proposed uses a classical FLASH device and only requires the fabrication of a suitable sample container with known dimensions and properties in which the sample is introduced. The main difference with the classical FLASH method concerns the computation of the conductivity from the experimental thermogram. Indeed, we have recourse to an identification procedure based on a 3-D simulation of the transient heat transfer in the axisymmetric composite sample. The modeling takes into account the disturbing influence of the container on the temperature of the backside and requires the knowledge of the dimensions and composition of the filled container. In our study, we use the gauss linearization method to identify the thermal conductivity.

We have analyzed the different sources of errors: uncertainties related to the accuracy of the measurement apparatus (temperature and time); validity of the hypotheses of the ideal model used for identification (purely conductive transfer, homogeneous sample); uncertainty concerning the dimensions and properties of the container. This allows us to evaluate the total error of measurement. In our case, the total uncertainty is lower than 5%.

Thereafter, we have applied our method to two liquids (water and ethanol) and one pasty material (polyacrylamid gel) whose thermal properties are accurately known. The results obtained by our method are in good agreement with literature data. Then, our method proves to be very practical for the measurement of thermal characteristics of materials used in various technological fields such as biology (biological tissues, blood, ...) or food industry (meat, yogurt, cheese, food gels ...).

References

[1] W.J. Parker, R.J. Jenkins, C.P. Butler, G.L. Abbot, FLASH method of determining thermal diffusivity, heat capacity and thermal conductivity, J. Appl. Phys. 32 (1961) 1679–1684.

[2] A. Degiovanni, Diffusivité et méthode flash, Rev. Gén. Thermique 185 (1977) 420–441.

[3] Z. Soilihi, A. Degiovanni, Influence de la non-linéarité dans la mesure de la diffusivité thermique par la méthode flash, Rev. Gén. Thermique 262 (1983) 649–660.

[4] R. Taylor, Construction of apparatus for heat pulse thermal diffusivity measurements from 300–3000 K, Sci. Instrum. 13 (1980) 1193–1199.

[5] R. Taylor, Heat pulse thermal diffusivity measurements, High Temperatures—High Pressures 11 (1979) 43–58.

[6] A. Degiovanni, J.-C. Batsale, D. Maillet, Mesure de la diffusivité longitudinale de matériaux anisotropes. Panorama des techniques développées au LEMTA, Rev. Gen. Thermique 35 (1996) 141–147.

[7] J.-C. Krapez, Mesure de diffusivité longitudinale de plaques minces par méthode de grille, in : Proceedings of Journée SFT « Thermographie IR quantitative », ONERA, 1999.

[8] M. Lafond-Huot, J. Bransier, Caractérisation thermocinétique des matériaux composites fibreux soumis à un flux de rayonnement impulsionnel, Lett. Heat Mass Transfer 9 (1982) 49–58.

[9] A.-M. Luc, D.L. Balageas, Comportement thermique des composites à renforcement orienté soumis à des flux impulsionnels, High Temperatures—High Pressures 16 (1984) 209–219.

[10] I. Philippi, J.-C. Batsale, D. Maillet, A. Degiovanni, Measurement of thermal diffusivity through processing of infrared images, Rev. Sci. Instrum. 66 (1995) 182–192.

[11] J.-C. Batsale, C. Gobbe, M. Quintard, Local non-equilibrium heat transfer in porous media, Recent Res. Devel. Heat, Mass Momentum Transfer 1 (1996).

[12] L. Ramond, J.-C. Batsale, C. Gobbe, M. Quintard, Measurement of a thermal exchange coefficient in porous media by infrared thermography—two temperature model application, in: Proceedings of 11th Int. Heat Transfer Conference, Kyong Ju Korea, 1998.

[13] L. Ramond, J.-C. Batsale, C. Gobbe, Méthodologie de mesure de coefficient d'échange en milieu poreux. Application d'un modèle à deux températures, Int. J. Thermal Sci. 38 (1999) 250–257.

[14] S. Azizi, J.-C. Batsale, C. Moyne, A. Degiovanni, Mesure de la conductivité thermique de milieux poreux non saturés : analyse théorique et expériences, High Temperatures—High Pressures 21 (1989) 383–389.

[15] C. Moyne, J.-C. Batsale, A. Degiovanni, Approche expérimentale théorique de la conductivité thermique des milieux poreux humides, Int. J. Heat Mass Transfer 31 (1988) 2305–2317.

[16] C. Moyne, J.-C. Batsale, A. Degiovanni, D. Maillet, Thermal conductivity of wet porous media: theoretical analysis and experimental measurements, in: C.J. Cremers, H.A. Fine (Eds.), Proceedings of Thermal Conductivity 21, Plenum Press, Lexington, Kentucky, 1990, pp. 109–120.

[17] S. André, A. Degiovanni, A theoretical study of the transient coupled conduction and radiation heat transfer in glass: phonic diffusivity measurements by the flash technique, Int. J. Heat Mass Transfer 38 (1995) 3401–3412.

[18] M. Lazard, S. André, D. Maillet, Diffusivity measurement of semi-transparent media: model of the coupled transient heat transfer and experiments on glass, silica glass and zinc selenide, Int. J. Heat Mass Transfer 47 (2004) 477–487.

[19] O. Hahn, F. Raether, M.C. Arduini-Schuster, J. Fricke, Transient coupled conductive/radiative heat transfer in absorbing, emitting and scattering media: application to laser-flash measurements on ceramic materials, Int. J. Heat Mass Transfer 40 (1997) 689–698.

[20] B. Le Neindre, Mesure de la conductivité thermique des liquides et des gaz, in : Techniques de l'Ingénieur, Mesures et contrôle (Tech. ing., Mes. contrôle), vol. RC3, n°R2920, 1996, pp. R2920.1–R2920.21.

[21] J.T. Schriempf, A laser flash technique for determining thermal diffusivity of liquid metals at elevated temperatures, Rev. Sci. Inst. 43 (1972) 781–786.

[22] M.M. Farooq, W.H. Giedt, N. Araki, Thermal diffusivity of liquids determined by flash heating of a three-layered cell, J. Thermophys. 1 (1981) 39–54.

[23] Y. Maeda, H. Sagara, R.P. Tye, M. Masuda, H. Ohta, Y. Waseda, A high-temperature system based on the laser flash method to measure the thermal diffusivity of melts, Int. J. Thermophys. 17 (1996) 253.

[24] T. Nishi, H. Ohta, H. Shibata, Y. Waseda, Evaluation of the heat leakage in the thermal diffusivity measurement of molten metals by a laser flash method, Int. J. Thermophys. 24 (2003) 1735–1751.

[25] Y. Tada, M. Harada, M. Tanigaki, E.Y. Eguchi, Laser flash method for measuring thermal conductivity of liquids—application to low thermal conductivity liquids, Rev. Sci. Inst. 49 (1978) 1305–1314.

[26] H. Ohta, H. Shibata, A. Suzuki, Y. Waseda, Novel laser flash technique to measure thermal effusivity of highly viscous liquids at high temperature, Rev. Sci. Inst. 72 (2001) 1899–1903.

[27] D. Segelstein, The complex refractive index of water, M.S. Thesis, University of Missouri–Kansas City, 1981.
[28] S. Ostrach, Natural convection in enclosures, J. Heat Transfer 110 (1988) 1175–1190.
[29] A. Dittmar, F. Arnaud, G. Delhomme, P. Girard, W.H. Newman, C. Martelet, Noninvasive characterization of skin using micro thermal diffusion sensor, in: Proceedings of 17th IEEE Engineering in Medicine and Biology Society Annual Conference, 1995.
[30] Y. Hirata, Y. Kato, N. Andoh, N. Fujiwara, R. Ito, Measurements of thermophysical properties of polyacrylamide gel used for electrophoreses, J. Chem. Engrg. Japan 26 (1993) 143–147.
[31] A. Faghri, Heat Pipe Science and Technology, Taylor and Francis, Bristol, 1995.